Journal of Thermal Engineering
Web page info: https://jten.yildiz.edu.tr
DOI: 10.18186/thermal.1285240

Research Article

Impact of the V CAP on induced turbulent air flow in a solar chimney: a computational study

Nguyen Minh PHU[1,*], Nguyen Hoang KHA[2], Nguyen Van HAP[2]

[1]*Faculty of Heat and Refrigeration Engineering, Industrial University of Ho Chi Minh City, Vietnam*
[2]*Faculty of Mechanical Engineering, Ho Chi Minh City University of Technology, VNU-HCM, Vietnam*

ARTICLE INFO

Article history
Received: 27 March 2021
Accepted: 10 May 2021

Keywords:
Solar Chimney; Natural Ventilation; CFD; Top Cap

ABSTRACT

In this paper, a 2D numerical simulation of a solar chimney with a top V cap was performed to evaluate the induced air flow degradation. Dimensions including the width of the cap and the cap offset from the top of chimney are specified as key parameters. Meanwhile, height and width of the chimney are fixed. The numerical model was confirmed to be accurate compared to the published data. The results showed that reducing the offset and increasing the width reduces airflow through the chimney. The effect of offset on chimney intake air is significant. When considering the addition of the top V cap, the airflow is reduced by about 20% compared to the chimney without a cap. This is because the cap forms three primary vortices including one vortex below the cap and two ones above the cap. The vortex under the cap in the direction from the absorber plate to the glass cover increases the air flow out of chimney at the side of the glass cover. The region with great turbulent kinetic energy forms at upper side of the cap. The air flow correlation as a function of the heat flux to the absorber plate, cap offset and cap width have been developed with errors of less than 2.5%.

Cite this article as: Phu N M, Kha N H, Hap N V. Impact of the V CAP on induced turbulent air flow in a solar chimney: a computational study. J Ther Eng 2023;9(2):510–517.

INTRODUCTION

Solar chimney is a simple and efficient natural ventilation device without pumping power. Its absorber surface receives solar radiation and heats the air which moves upwards via the chimney effect. It is suitable for natural ventilation purposes in living spaces or farms in the areas where radiation intensity is high and stable. The different configurations of solar chimney have been studied experimentally, numerically or analytically to evaluate performance. Very early, Ong [1] proposed a simple analytical model based on the flat plate collector theory. The model is the basis for next predictive models that have taken into account corrections to improve accuracy. Chen et al. [2] have experimentally investigated the vertical and inclined solar chimneys. They found that the 45° tilt angle provides the greatest air flow and is 45% higher than that of a vertical chimney. Bassiouny and Koura [3] investigated and analyzed a solar

***Corresponding author.**
*E-mail address: nguyenminhphu@iuh.edu.vn

This paper was recommended for publication in revised form by Regional Editor Omid Mahian

chimney coupled with a ventilated room. They reported that the effect of chimney width was more important than inlet size and suggested chamfering chimney inlet. Arce et al. [4] have experimentally surveyed a solar chimney to determine the discharge coefficient. The coefficient was defined as 0.52 which is useful for designing a solar chimney. Manca et al. [5] has simulated a vertical solar chimney with inclined glass. They confirmed that the air flow increased by 20% compared with the vertical glass cover. Khanal and Lei [6] determined the optimal angle of 4° to achieve maximum flow rate. In addition, they claimed that increasing inclination of solar chimney reduces turbulence kinetic energy and turbulence intensity. Exergetic analysis of a solar chimney was done by López et al. [7]. They demonstrated that the exergy performance of a solar chimney is very low and suggested improving this performance by changing the design. Jing et al. [8] experimentally evaluated the effect of solar chimney with large air gap on induced air flow. They conclude that the existing mathematical model exhibited a poor prediction, especially cases with a large chimney width. They modified the model by considering the reversed flow at the chimney outlet to improve accuracy. Recently, Duan [9] developed a new analytical model to predict air flow and air temperature difference across solar chimney. The prediction of this model has been compared with the experimental results with acceptable errors. More recently, Xamán et al. [10] evaluated a solar chimney in conjunction with a ventilated room. They showed that ventilation effectiveness was improved up to 45% and air change per hour up to 2.5. Kong et al. [11] simulated solar chimneys that were tilted 30 to 90° relative to the horizontal plane. They found that inclination angles from 45 to 60° achieved the greatest discharge depending on season and latitude. Nguyen and Wells [12] numerically investigated of horizontal solar chimneys. They concluded that outlet width had a notable effect on the thermal efficiency of a solar chimney. The efficiency dropped drastically from 90% to 30% when increasing outlet width beyond a specific dimension.

The air outlet of a solar chimney is located outdoor. Therefore, it is obvious that a cap must be installed to protect against weather conditions such as rain, snow or bird waste. This cap results in a decrease in the natural ventilation air flow due to the effect of an obstruction at the exit. An evaluation of the effect of top retrofitted cap on induced air flow has not been found in open literature. Thus, this study investigates the effect of the position and size of the V-shaped cap on the air flow and temperature distribution of a vertical chimney by 2D numerical analysis using the commercial code ANSYS-Fluent.

MODEL DESCRIPTION AND VALIDATION

Figure 1 shows a solar chimney with the height of 521 mm and the air gap of 40 mm studied in this paper. The

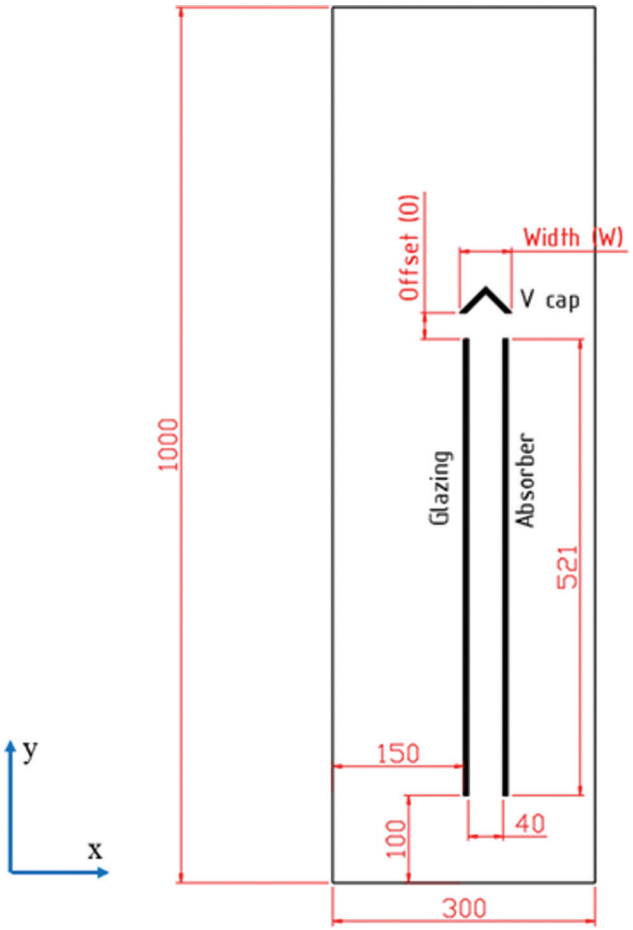

Figure 1. Dimensions of the computational domain (mm).

right wall is glass cover and the left wall is the absorber plate. These dimensions were adopted from the previous study [11] to verify and compare. On the top of chimney there is a right-angle V cap with an offset (O) from chimney and a width (W). In this study, O varies between 40 and 60 mm, W in the range of 65 to 75 mm and the heat flux received from solar radiation of the absorber plate from 200 to 800 W/m^2. To simulate the flow of air entering and leaving the chimney, the calculated domain is extended to a rectangle of 300 mm ´ 1000 mm. Figure 2 shows the meshing of the computational domain in which the absorber surface and the glass surface are refined for intensifying predictive accuracy.

The problem of natural convection in open domain was numerically solved using the SST k-w turbulence model and the DO (Discrete Ordinates) radiative heat transfer model [11] in the ANSYS Fluent 18.2 simulation tool. The governing equations have been presented in the ANSYS Fluent manual so they are not presented here for simplicity [13-17]. The governing equations have been solved with the assignment of boundary conditions as shown in Table

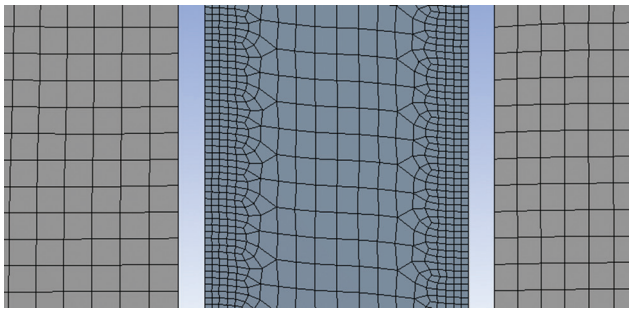

Figure 2. Meshing of the domain with refinement for inner walls of the chimney.

1. Equations (1)-(6) summarize the governing equations in two-dimensional form.

Continuity equation:

$$\nabla\cdot(\rho\vec{v})=0 \tag{1}$$

Momentum equation:

$$\nabla\cdot(\rho\vec{v}\vec{v})=-\nabla P+\nabla\cdot\vec{\tau}+\rho\vec{g} \tag{2}$$

Energy equation:

$$\nabla\cdot\left[\vec{v}(\rho E+P)\right]=\nabla\cdot\left(k_{\text{eff}}\right)\nabla T+\nabla\cdot(\vec{\tau}\vec{v}) \tag{3}$$

Turbulence kinetic energy equation:

$$\frac{\partial}{\partial x_i}(\rho k u_i)=\frac{\partial}{\partial x_j}\left(\Gamma_k\frac{\partial k}{\partial x_j}\right)+G_k-Y_k+S_k \tag{4}$$

Dissipation rate equation:

$$\frac{\partial}{\partial x_j}(\rho\omega u_j)=\frac{\partial}{\partial x_j}\left(\Gamma_\omega\frac{\partial\omega}{\partial x_j}\right)+G_\omega-Y_\omega+S_\omega+D_\omega +C_{3\varepsilon}G_b-C_{2\varepsilon}\rho\frac{\varepsilon^2}{k}+S_\varepsilon \tag{5}$$

Radiative transfer equation of DO model:

$$\nabla\cdot\left[I(\vec{r},\vec{s})\vec{s}\right]+(a_c+\sigma_s)I(\vec{r},\vec{s}) =a_c n^2\frac{\sigma T^4}{\pi}+\frac{\sigma_s}{4\pi}\int_0^{4\pi}I(\vec{r},\vec{s}')\phi(\vec{s},\vec{s}')d\Omega' \tag{6}$$

To deal with temperature-dependent density of air, ideal gas was assumed in the present study. The PRESTO! Scheme was employed to pressure term for catching up the buoyancy-driven problem [13, 18]. The errors for all governing equations are assigned as 10^{-4} for the convergence. Figure 3 shows the grid independence test for the case without a cap at heat flux of 800 W/m^2. The tested number of meshes ranged from 14338 to 79859 elements. It can be seen clearly that when the mesh number is 36810 or more, the velocity profile at the chimney outlet does not change significantly. Therefore, the settings at this grid number are applied to all studied cases. Figure 4 shows the distribution of y^+ value along the walls of the chimney. The average y^+ of the glass wall and absorber plate reached 1.24 which was close to 1 as suggested by Kong et al. 2020 [11]. A further decrease in y^+ increases the induced airflow negligibly. However, the computation time significantly increases.

To confirm the results from the numerical methodology, the air flow at the chimney outlet in the absence of a cap is compared with published data with the same chimney height and chimney gap. Figure 5 shows the effect of the received heat of the absorber plate on the sucked air flow per 1 m of spanwise width. It can see a good agreement

Table 1. Boundary conditions

Wall	Boundary conditions
Bottom wall of computational domain	Pressure inlet, 300 K, 101325 Pa
Right wall of computational domain	Pressure inlet, 300 K, 101325 Pa
Left wall of computational domain	Pressure outlet, 300 K, 101325 Pa
Top wall of computational domain	Pressure outlet, 300 K, 101325 Pa
Glazing wall	No-slip conditions, emissivity = 0.86
Absorber wall	No-slip conditions, emissivity = 0.95, heat flux = 200 to 800 W/m^2

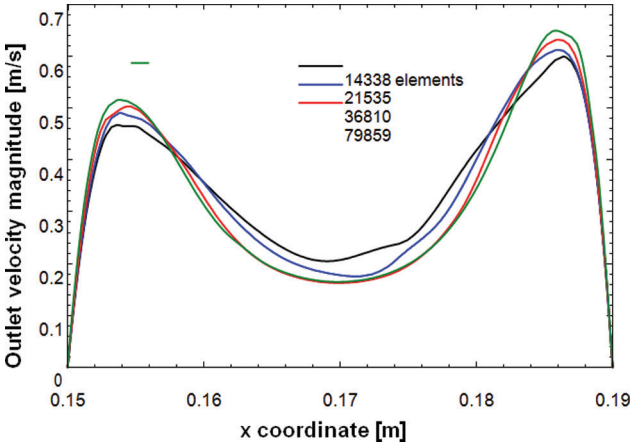

Figure 3. Grid independence test.

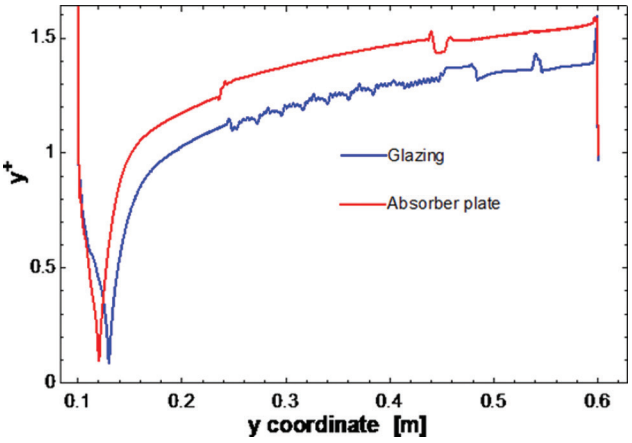

Figure 4. Dimensionless wall distance (y^+) along glazing and absorber plate.

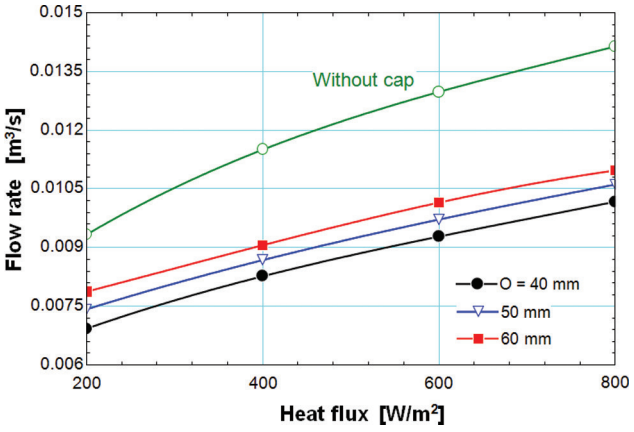

Figure 6. Effects of heat flux and V cap offset at W = 70 mm.

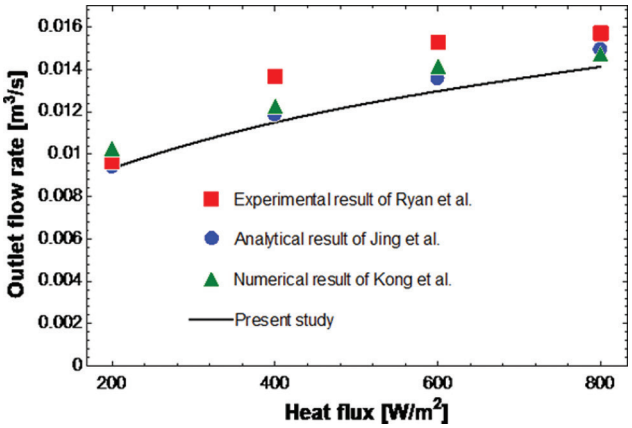

Figure 5. Validation with experimental result [19], analytical result [8], and numerical simulation result [11].

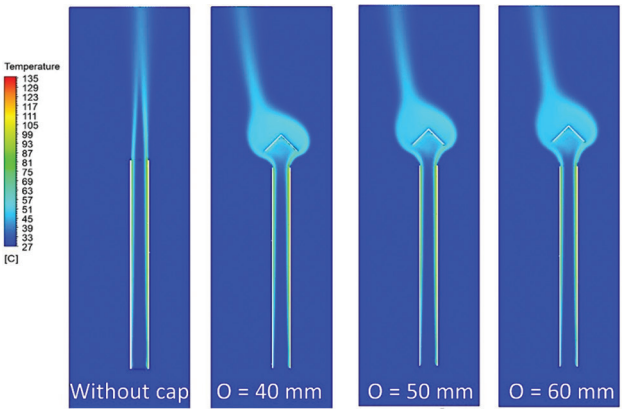

Figure 7. Temperature distribution with V cap offsets at q= 800 W/m² and W=75 mm.

between current simulation results with experimental, theoretical and simulated results in previous studies. The maximum errors of current research with analytical, simulated and experimental results are 5.4%, 9.2% and 15.8%, respectively. From this confirmation, simulation of the effect of V cap at top of the chimney was conducted to evaluate the flow rate and perform further analyzes in the next section.

RESULTS AND DISCUSSION

The effects of the cap offset and heat flux on the intake air flow are shown in Figure 6 at fixed cap width of 70 mm. The airflow rate of the chimney without cap has also been plotted for the sake of comparison. It can be seen that due to the interference of the cap, the solar chimney with a cap has air flow rate about 20% lower than the no cap case. When the offset increases, the air inside the chimney is easy to escape, so the induced flow increases.

Figure 7 shows the air temperature distribution in the computational domain at the same heat flux and cap width. The air temperature at chimney core is close to the ambient temperature, the highest air temperature is near the absorber plate followed by the glass cover due to the transfer of radiant heat from the absorber plate to the glass cover. The air temperature around the cap with the smallest offset has the highest value. Due to the small offset, a low air flow results in a larger air temperature. The higher air, the lower is air temperature due to diffusion of the hot air with the cold air in the environment.

Figure 8 shows the air velocity magnitude at a heat flux of 800 W/m². The air flow rate in the chimney without cap is significantly larger than the actual chimney having a cap. The inlet velocity profile is quite similar between the

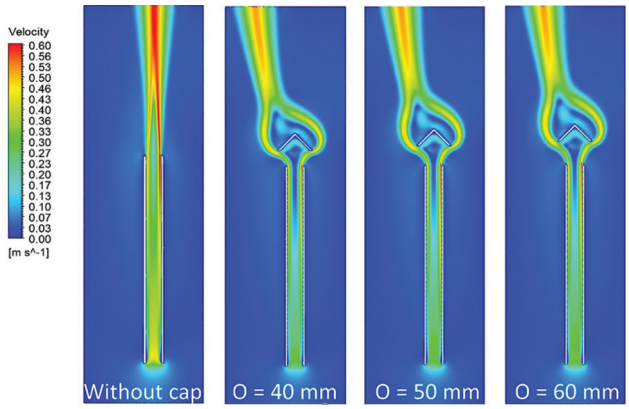

Figure 8. Velocity magnitude with V cap offsets at q = 800 W/m^2 and W =75 mm.

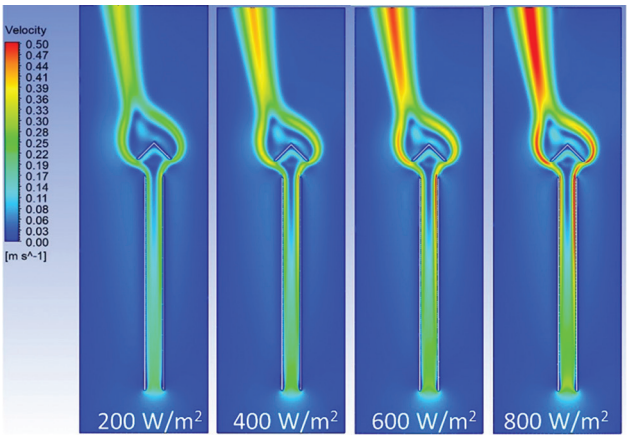

Figure 10. Velocity magnitude variation with heat fluxes at O = 40 mm and W = 70 mm.

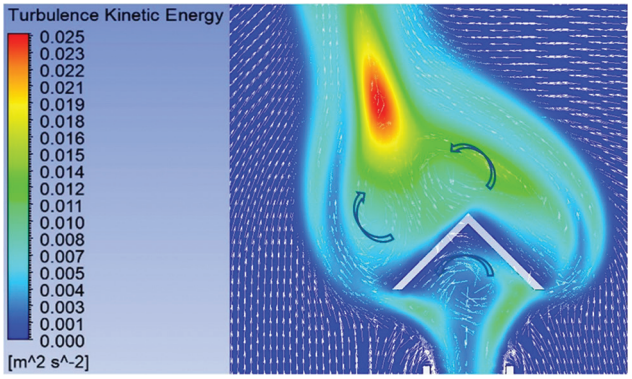

Figure 9. Turbulence kinetic energy and velocity vector around a V cap.

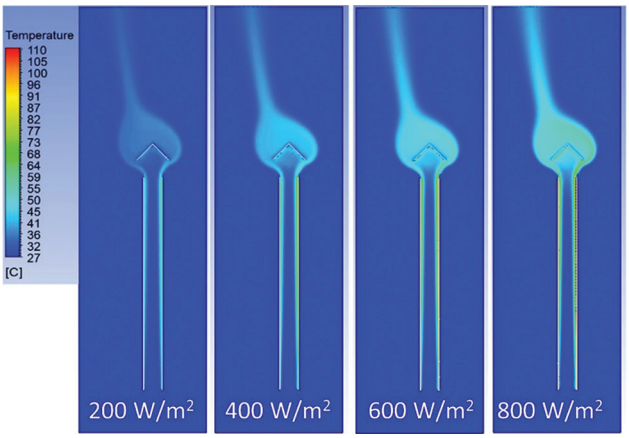

Figure 11. Temperature distribution by varying heat flux at O = 40 mm and W=70 mm.

presence and absence of a cap. However, in the last half of the chimney, the chimney core has almost no air moving because the V-shape of the cap causes the large static pressure field below the cap. This results in a reduction in the intake air flow.

Figure 9 clarifies the flow mechanism around V cap via velocity vector and turbulence kinetic energy contour. A moving stream of air can be seen below the cap from the absorber plate to the glass cover. This is because the air near the plate absorbs thermal energy of the highest temperature surface resulting in maximum velocity. This high velocity flow is blocked and guided by the wall of the cap so it moves towards the glass cover. This can lead to the outflow from the left side higher than the right side as can be seen in Figure 6. This explains the fact that the air current above the cap tends to blow to the left. Above the cap, there is a vortex pair formed from two streams coming out of chimney. This causes the largest turbulence kinetic energy region like vortex shedding from a fluid moving past an obstruction. In the absence of a cap, the largest turbulence kinetic energy is probably in the airflow leaving the chimney from the side of the absorber plate followed by the glass side. For a solar chimney without cap, Khanal and Lei [6] showed that the highest turbulence intensity occurred at the chimney exit close to the absorber plate. The current study coincides well with their observations. However, when a V-shaped cap is installed, the region with the highest turbulence intensity occurs at the downstream of the cap.

Figures 10 and 11 show the velocity magnitudes and isotherms at different heat fluxes; meanwhile, the geometries of the cap are fixed. It can be seen clearly that increasing solar thermal energy to the absorber plate, the temperatures of air and surfaces inside the chimney raise monotonically. The increased temperature of absorber plate and glass cover leads to augment the buoyancy driven natural convection current.

The effect of cap width on air flow is shown in Figure 12. It can be seen that when increasing cap width, it reduces the cross-sectional area for escaping the induced air out of solar chimney. However, the effect of cap width on the air flow is negligible compared to heat flux and offset.

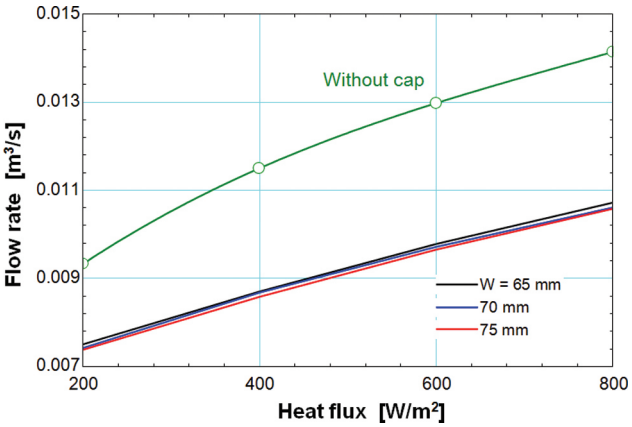

Figure 12. Effects of cap width at O = 50 mm.

In order to facilitate the design and evaluation of the effects of the parameters on the ventilation air flow rate, the flow function according to the three variables examined above including heat flux, cap offset and cap width was developed upon linear regression. The development steps are illustrated in Figures 13a-c regarding to the sequential plot of the variables [20]. The results obtained the air flow correlation as equation (7). To confirm the accuracy of the predictive equation, Figure 13d shows the prediction result from equation 7 and input data. The results reveal that the equation has good predictability with errors less than 2.5%. From the exponents of the function, it can be seen that the effect of offset is equivalent to the absorption heat flux gained from solar radiation and the effect of cap width is less significant.

$$\dot{V}_{predicted} = 0.00112172421 q^{0.25661058} O^{0.238275349} W^{-0.0964393807} \quad (7)$$

The equation (7) is applicable with the following parameters:

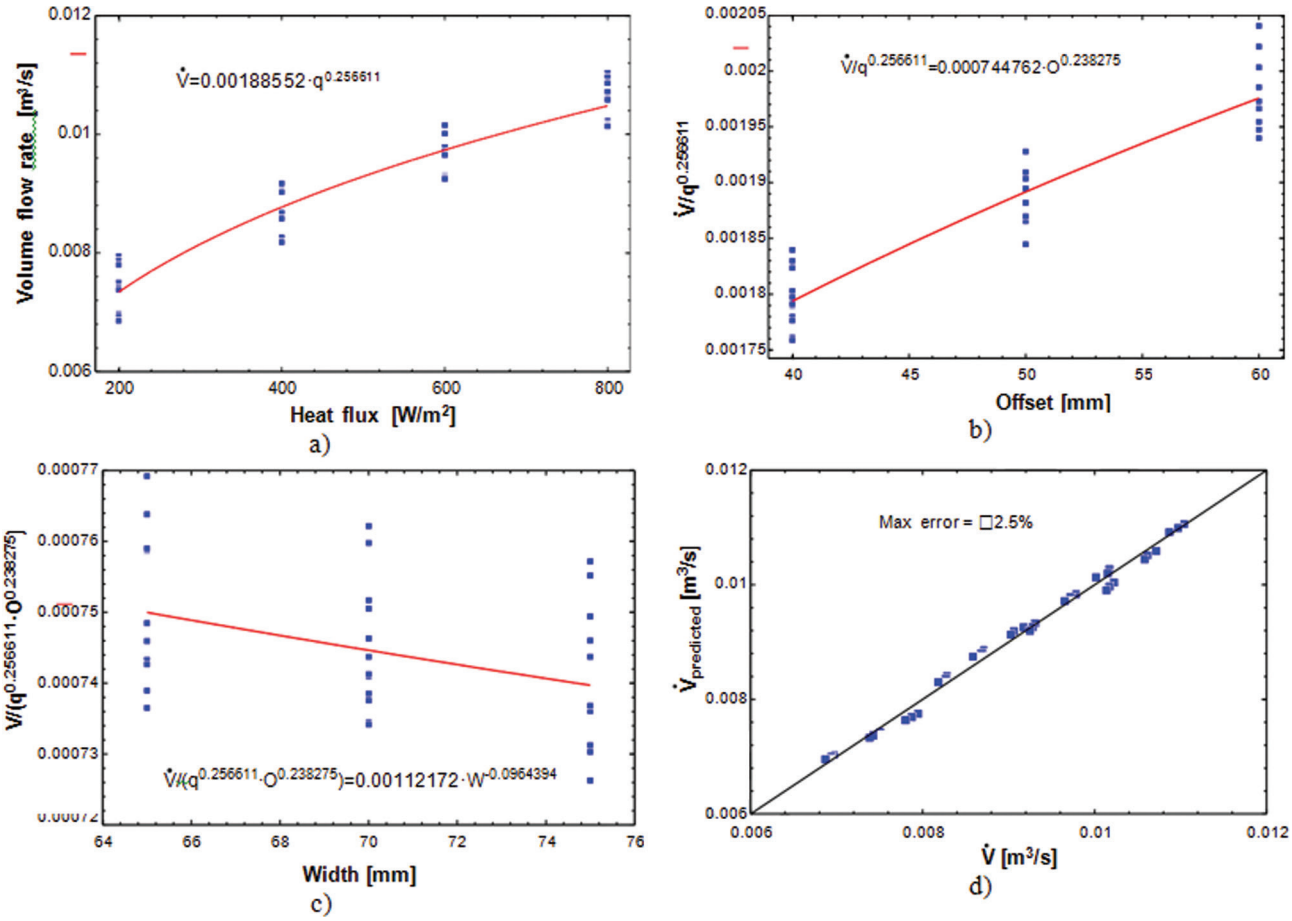

Figure 13. Correlation development of induced air flow with the examined variables.

- Solar chimney height of 521 mm
- Solar chimney gap of 40 mm
- Heat flux (q) from 200 to 800 W/m^2
- Cap offset (O) from 40 to 60 mm
- Cap width (W) from 65 to 75 mm

Figure 3 shows a transparent enclosure includes a particulate (participating) media. This figure describes the radiative phenomena inside a particulate media. When radiative energy travels through participating media, the incident beams are attenuated by scattering and absorption, while others are transmitted through this media to the other side.

CONCLUSION

Effects of position and size of a V-shaped cap on the performance of a solar chimney are presented in this paper. A 2D numerical simulation used the SST k-w turbulence model and the DO radiation model to determine temperature distribution, air velocity, and induced air flow. The results show that the cap shield reduces air flow about 20%. The effect of cap offset on ventilation flow rate is more significant than that of cap width. There is a vortex below the cap in the direction from the absorber plate to the glass cover due to the higher temperature of the absorber plate resulting in a higher air velocity on the side of the glass cover. Two large vortices are observed at downstream of the cap that causes the energy loss of buoyancy-driven flow. A linear regression function of the induced air flow with independent variables of heat flux, cap offset and cap width was developed to quantify the influencing factors and facilitate the design and selection of cap shield for solar chimney.

From the current research results, it is suggested that the design of natural ventilation using solar thermal energy should take into account the reduction in air flow caused by chimney cap. Also, the different configurations of solar chimney, i.e., inclined glazing, inclined absorber plate, horizontal chimney should be evaluated with respect to congested free convection current.

NOMENCLATURE

O	Cap offset (mm)
P	Pressure (Pa)
q	Heat flux (W/m^2)
T	Temperature (°C)
$\dot{V}$	Volume flow rate (m^3/s)
$\vec{v}$	Velocity vector (m/s)
W	Cap width (mm)
x	Horizontal coordinate
y	Vertical coordinate
y^+	Dimensionless wall distance

Greek symbol

r	Density (kg/m^3)

ACKNOWLEDGMENTS

This research is funded by the Vietnam National University Ho Chi Minh City (VNU-HCM) under grant number B2021-20-06.

AUTHORSHIP CONTRIBUTIONS

Authors equally contributed to this work.

DATA AVAILABILITY STATEMENT

The authors confirm that the data that supports the findings of this study are available within the article. Raw data that support the finding of this study are available from the corresponding author, upon reasonable request.

CONFLICT OF INTEREST

The author declared no potential conflicts of interest with respect to the research, authorship, and/or publication of this article.

ETHICS

There are no ethical issues with the publication of this manuscript.

REFERENCES

[1] Ong KS. A mathematical model of a solar chimney. Renew Energy 2003;28:1047–1060. [CrossRef]

[2] Chen ZD, Bandopadhayay P, Halldorsson J, Byrjalsen C, Heiselberg P, Li Y. An experimental investigation of a solar chimney model with uniform wall heat flux. Build Environ 2003;38:893–906. [CrossRef]

[3] Bassiouny R, Koura NSA. An analytical and numerical study of solar chimney use for room natural ventilation. Energy Build 2008;40:865–873. [CrossRef]

[4] Arce J, Jiménez MJ, Guzmán JD, Heras MR, Alvarez G, Xamán J. Experimental study for natural ventilation on a solar chimney. Renew Energy 2009;34:2928–2934. [CrossRef]

[5] Manca O, Nardini S, Romano P, Mihailov E. Numerical investigation of thermal and fluid dynamic behavior of solar chimney building systems. J Univ Chem Technol Metallurgy 2014;49:106–116.

[6] Khanal R, Lei C. A numerical investigation of buoyancy induced turbulent air flow in an inclined passive wall solar chimney for natural ventilation. Energy Build 2015;93:217–226. [CrossRef]

[7] Suárez–López MJ, Blanco–Marigorta AM, Gutiérrez–Trashorras AJ, Pistono–Favero J, Blanco–Marigorta E. Numerical simulation and exergetic

analysis of building ventilation solar chimneys. Energy Convers Manag 2015;96:1–11. [CrossRef]

[8] Jing H, Chen Z, Li A. Experimental study of the prediction of the ventilation flow rate through solar chimney with large gap–to–height ratios. Build Environ 2015;89:150–159. [CrossRef]

[9] Duan S. A predictive model for airflow in a typical solar chimney based on solar radiation. J Build Eng 2019;26:100916. [CrossRef]

[10] Jiménez–Xamán C, Xamán J, Gijón–Rivera M, Zavala–Guillén I, Noh–Pat F, Simá E. Assessing the thermal performance of a rooftop solar chimney attached to a single room. J Build Eng 2020;31:101380. [CrossRef]

[11] Kong J, Niu J, Lei C. A CFD based approach for determining the optimum inclination angle of a roof–top solar chimney for building ventilation. Sol Energy 2020;198:555–569. [CrossRef]

[12] Nguyen YQ, Wells JC. A numerical study on induced flowrate and thermal efficiency of a solar chimney with horizontal absorber surface for ventilation of buildings. J Build Eng 2020;28:101050. [CrossRef]

[13] Fluent Inc, FLUENT User's Guide, New Hampshire, USA, 2017.

[14] Ngo TT, Go J, Zhou T, Nguyen HV, Lee GS. Enhancement of exit flow uniformity by modifying the shape of a gas torch to obtain a uniform temperature distribution on a steel plate during preheating. Appl Sci 2018;8:2197. [CrossRef]

[15] Ngo TT, Zhou T, Go J, Nguyen HV, Lee GS. Improvement of the steel–plate temperature during preheating by using guide vanes to focus the flame at the outlet of a gas torch. Energies 2019;12:869. [CrossRef]

[16] Mai TD, Ryu J. Effects of leading–edge modification in damaged rotor blades on aerodynamic characteristics of high–pressure gas turbine. Mathematics 2020;8:2191. [CrossRef]

[17] Mai TD, Ryu J. Effects of damaged rotor blades on the aerodynamic behavior and heat–transfer characteristics of high–pressure gas turbines. Mathematics 2021;9:627. [CrossRef]

[18] Phu NM, Van Hap N. Numerical Investigation of Natural Convection and Entropy Generation of Water near Density Inversion in a Cavity Having Circular and Elliptical Body. In: Ghaedi K, Alhusseny A, Nasser A, Al-Zurf N, editors. Fluid–structure interaction. 1st ed. London: IntechOpen; 2020. pp. 1–13.

[19] Ryan D. Experimental investigation of buoyancy driven natural convection for solar applications in building facades. Doctoral Thesis. Scotland: Glasgow Caledonian Univ; 2008.

[20] Luan NT, Phu NM. Thermohydraulic correlations and exergy analysis of a solar air heater duct with inclined baffles. Case Stud Therm Eng 2020;21:100672. [CrossRef]